Environmental Science & Technology

Article

pubs.acs.org/est

Application and Validation of an Impedance-Based Real Time Cell Analyzer to Measure the Toxicity of Nanoparticles Impacting Human Bronchial Epithelial Cells

Lila Otero-González,[†] Reyes Sierra-Alvarez,*[,†] Scott Boitano,[‡] and Jim A. Field[†]

[†]Department of Chemical & Environmental Engineering and [‡]Department of Physiology, The University of Arizona, Tucson, Arizona 85721, United States

Supporting Information

ABSTRACT: Nanomaterials are increasingly used in a variety of industrial processes and consumer products. There are growing concerns about the potential impacts for public health and environment of engineered nanoparticles. The aim of this work was to evaluate a novel impedance-based real time cell analyzer (RTCA) as a high-throughput method for screening the cytotoxicity of nanoparticles and to validate the RTCA results using a conventional cytotoxicity test (MTT). A collection of 11 inorganic nanomaterials (Ag^0, Al_2O_3, CeO_2, Fe^0, Fe_2O_3, HfO_2, Mn_2O_3, SiO_2, TiO_2, ZnO, and ZrO_2) were tested for potential cytotoxicity to a human bronchial epithelial cell, 16HBE14o-. The data collected by the RTCA system was compared to results obtained using a more traditional methyl tetrazolium (MTT) cytotoxicity assay at selected time points following application of nanomaterials. The most toxic nanoparticles were ZnO, Mn_2O_3 and Ag^0, with 50% response at concentrations lower than 75 mg/L. There was a good correlation in cytotoxicity measurements between the two methods; however, the RTCA method maintained a distinct advantage in continually following cytotoxicity over time. The results demonstrate the potential and validity of the impedance-based RTCA technique to rapidly screen for nanoparticle toxicity.

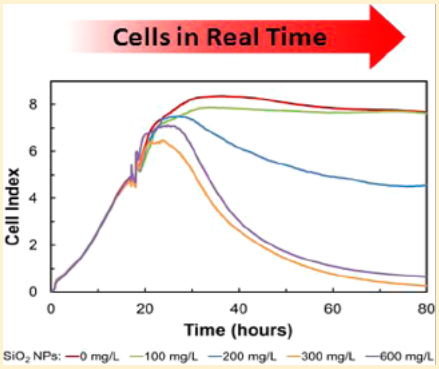

INTRODUCTION

Engineered nanomaterials are characterized by having less than 100 nm in at least one dimension. The small size confers nanomaterials with unique properties that have been exploited in multiple applications. Nanotechnology is a continuously expanding field that is expected to achieve a global market value of over $ US 2 trillion by 2015.[1] Inorganic nanoparticles (NPs) are among the most commonly used engineered nanomaterials. The field of application of these NPs is very wide, including sunscreens and cosmetics (ZnO, TiO_2), bactericidal products (Ag^0), environmental remediation technologies (Fe^0, TiO_2), catalysis (Mn_2O_3), and used in the semiconductor industry (CeO_2, Al_2O_3, SiO_2), among others.[2−4] The growth in utilization of engineered nanomaterials has led to an increase in the release of NPs to the environment,[5] raising concerns about their potential hazards to human health and the environment.

The concerns make an evaluation of the potential toxicity of NPs imperative; however, there are some methodological problems when assessing NPs toxicity. For example, some NPs can interfere with classical end-point methods which are dependent on colorimetric or fluorimetric measurements. For instance, single-walled carbon nanotubes (SWCNT) are known to bind MTT-formazan so that the crystals cannot be solubilized, leading to false positive results.[6] Mesoporous SiO_2 NPs also interfere with the MTT test enhancing the exocytosis of the MTT-formazan in HeLa cells and astrocytes.[7] Absorption of fluorescence by carbon black NPs was observed when using the dichlorofluorescein dye to detect formation of reactive oxygen species (ROS).[8] To avoid issues associated with the interference of NPs, we propose the use of a novel label-free and impedance-based system as a high throughput technique for nanotoxicity screening and assessment.[9]

The real time cell analyzer (RTCA) system measures the electrical impedance across interdigitated microelectrodes integrated on the bottom of 96-well tissue culture plates (E-plates).[9] The impedance measured is affected by the biological status of the cells interacting with the well surface. Cells that interact with the electrode modify the local ionic environment and lead to an increase in the impedance measured within the tissue culture well. Thus, the electrode impedance can be used to monitor cell number, viability, morphology, and adhesion degree.[10] The impedance is displayed as the cell index (CI) value, which is a dimensionless parameter calculated by

$$CI = \max_{i=1,\ldots,N}\left[\frac{R_{cell}(f_i)}{R_b(f_i)} - 1\right] \quad (1)$$

Received: April 21, 2012
Revised: August 22, 2012
Accepted: August 23, 2012
Published: August 23, 2012

where $R_{cell}(f_i)$ is frequency-dependent electrode impedance at any time, $R_b(f_i)$ is background impedance measured at the initial time without cells, and N is number of the frequency points at which the impedance is measured.

The RTCA method has several advantages over classical methods. First, it is label free, so the potential interference of NPs with fluorescent or colorimetric dyes can be avoided. Second, it is noninvasive and thus does not interfere with the normal cell metabolism nor mandate a single time point measurement. Third, it is a high-throughput technique, enabling significantly larger data acquisition than that obtained using a traditional end-point assay. Compared to other high-throughput methods recently applied to nanotoxicity assessment such as DNA microarrays and platforms to screen for lethal and sublethal injury responses (e.g., ATP content, membrane permeability, reactive oxygen species, etc.),[11] the RTCA system has as an advantage the ability to monitor dynamic responses in real time. Despite these significant advantages, demonstrated by use of RTCA in cytotoxicity screening of soluble compounds, only limited information is available on the applicability of the RTCA system to nanoparticulate materials. Cell-electronic sensing was successfully applied to evaluate responses induced by microparticles such as quartz, urban air dust, and diesel particulates.[12] Recently the RTCA system has emerged as a potential alternative for nanotoxicity assessment. Preliminary studies have tested the applicability of the system for cytotoxicity assessment of CdTe quantum dots, iron/carbon, and SiO_2 NPs.[13−15]

The aim of this study is to evaluate the applicability of the RTCA system for high-throughput toxicity assessment of inorganic nanoparticles. To this end, 11 inorganic NPs were tested for potential cytotoxicity to human bronchial epithelial cells (16HBE14o-) using RTCA and results were compared to those obtained using a common physiological end-point assay (MTT).

EXPERIMENTAL SECTION

Nanoparticles. Ag^0 (99.5% purity), Al_2O_3 (99%), CeO_2 (99.95%), and SiO_2 (99.5%) were purchased from Sigma-Aldrich (St. Louis, MO). Fe^0 (99.9%), Fe_2O_3 (99%), Mn_2O_3 (98%), ZnO (99.8%), and ZrO_2 (99%) were acquired from SkySpring Nanomaterials Inc. (Houston, TX), and HfO_2 (99.9%) from American Elements (Los Angeles, CA). TiO_2 (99.5%) was a gift from Aerosil (Parsippany, NJ). All NPs were obtained as dry powders. Transmission electron micrographs (TEM) of the various nanomaterials investigated are provided in the Supporting Information (SI) section.

Nanoparticles Dispersions. NPs were dispersed in deionized (DI) water at a typical concentration of 4000 mg/L for cytotoxicity assays and 2000 mg/L for stability/aggregation assays. All dispersions were sonicated using a 130-W ultrasonic processor (Cole-Parmer Instruments, Vernon Hills, IL) at 70% amplitude for 5 min. The pH of the NP stocks was adjusted to 6−7 using diluted NaOH or HCl, as required. Stock dispersions were stored at 4 °C for no more than 24 h and sonicated for 5 min directly before use.

Cell Culture. 16HBE14o-, an adherent, immortalized human bronchial epithelial cell line,[16] was obtained through the California Pacific Medical Center Research Institute (San Francisco, CA). 16HBE14o- cells were initially grown as previously described.[17] Briefly, cells were grown in tissue culture flasks coated with a collagen/fibronectin bovine (CFB) serum albumin external matrix (88% LHC basal medium, 10% bovine serum albumin (BSA), 1% bovine collagen type I, and 1% human fibronectin) in a full growth medium that consisted of minimum essential medium with Earls' salts (MEM) supplemented with 10% (v/v) fetal bovine serum (FBS), 2 mM glutamax, penicillin and streptomycin at 37 °C in a 5% CO_2 humidified atmosphere. Subsequently, the medium was replaced by a low serum medium containing 5% FBS and cells were transferred to assay plates.

RTCA Assay. Cells were plated onto 96-well E-plates (Roche Applied Sciences, Indianapolis, IN) coated with CFB at a density of ∼510 000 cells/cm^2 (∼100 000 cells/well) in a low serum medium with 5% FBS and incubated for 15−16 h (37 °C, 5% CO_2). The impedance of each well was monitored using the RTCA device (xCELLigence, ACEA Biosciences, San Diego, CA). After the growth period, the culture medium was removed and cells were washed twice with fresh medium. Low serum medium (100 μL) was added to each well, and cells were incubated until the impedance signal was stable. Then cells were supplemented with the appropriate dose of NPs (100 μL). These NP dispersions were prepared a few minutes prior to their addition by diluting the NP stock (200 μL) with MEM containing 5% FBS (200 μL) (so the final ratio medium:NPs stock in the culture wells was 3:1, v/v). Cells were incubated for no less than 48 h. Assays were performed at least in quadruplicate and cell-free controls with the maximum concentration of NPs tested as well as NP-free controls were run in parallel.

The CI values for each well were expressed as normalized CI (NCI) for further calculations as

$$\mathrm{NCI}_i = \frac{\mathrm{CI}_i(t)}{\mathrm{CI}_i(t \text{ of dose})} \tag{2}$$

where $\mathrm{CI}_i(t)$ is CI at any time and $\mathrm{CI}_i(t$ of dose) is CI at the time of NPs dosing. The percentage of response, normalized to that of the NP-free control, was calculated after 48 h of exposure to NPs, using eq 3

$$\text{response}(\%) = \frac{\mathrm{NCI}(\text{treatment})}{\mathrm{NCI}(\text{control})} \times 100 \tag{3}$$

The NP concentrations resulting in 50% loss of cell index were calculated by interpolation in the graphs plotting the normalized response activity (%) as a function of the NP concentration.

MTT Assay. Cells were plated onto 12-well plates (Becton-Dickinson, Franklin Lakes, NJ) coated with CFB at a density of ∼130 000 cells/cm^2 (∼500 000 cells/well) in a low serum medium with 5% FBS and incubated (37 °C, 5% CO_2) for 24 h. The spent medium was removed, new low serum medium (750 μL) was added and cells received a 250 μL dose of target NPs. Sterile DI water (250 μL) was added to the NP-free control. Cell-free controls with the maximum concentration of NPs tested were also included. After 48 h of incubation, cells were washed twice with sterile 1× PBS (8 g/L NaCl, 0.2 g/L KCl, 1.44 g/L Na_2HPO_4, 0.24 g/L KH_2PO_4; pH= 7.4), MTT work solution (1 mL) was added to a final concentration of 0.4 g/L and plates were incubated at 37 °C for 1 h. The medium was removed and 1 mL of dimethyl sulfoxide (DMSO) was added to dissolve the formazan crystals. The optical density of the samples was measured at a wavelength of 550 nm.

The remaining mitochondrial activity was calculated as

$$\text{activity}(\%) = \frac{\text{absorbance(treatment)} - \text{absorbance(blank)}}{\text{absorbance(control)} - \text{absorbance(blank)}} \times 100 \quad (4)$$

The concentrations of the target NP causing 50% inhibition were calculated by interpolation in the graphs plotting the remaining activity (%) as a function of the NP concentration.

Stability of Nanoparticles in Dispersion. The stability of NPs in the culture medium was assessed by determining the particle size distribution (PSD) and zeta potential (ζ-potential) of cell-free samples following incubation (37 °C, 5% CO_2, 24 h). Samples (8 mL) of the NP stock diluted in low serum medium (1:3, v/v) were incubated in 15 mL conical-bottom polypropylene tubes. Samples of supernatant and the whole mixed dispersion were collected and analyzed for PSD, ζ-potential, and the concentration of the corresponding element.

Particle Size Distribution and Zeta Potential Measurements. The ζ-potential of NPs dispersions was measured with a ZetaSizer Nano ZS (Malvern, Inc., Sirouthborough, MA). PSD measurements were performed by dynamic light scattering (DLS) using the same instrument.

Analytical Methods. Prior to the determination of metal content, NP samples were subjected to microwave-assisted acid digestion (MARS System, CEM Corp., Matthews, NC), except Fe^0, Fe_2O_3, Mn_2O_3 and ZnO samples which were digested at room temperature. Liquid samples (1 mL) were mixed with a suitable digestion solution (see Supporting Information). Dissolved metals were measured by inductively coupled plasma-optimal emission spectroscopy (Optima 2100 DV, Perkin–Elmer, Shelton, CT), with the exception of Fe which was analyzed using the phenanthroline method (3500-Fe).[18]

RESULTS AND DISCUSSION

Cytotoxicity Assessment Using the RTCA System. The potential cytotoxicity of 11 widely used inorganic NPs to human bronchial epithelial cells (16HBE14o-) was evaluated using the impedance-based RTCA system. The cytotoxic effect, measured as loss of cell index (CI), was markedly different depending on the NP tested. Application of CeO_2, TiO_2, HfO_2, ZrO_2, and Fe_2O_3 nanoparticles did not show any toxicity, even at high concentrations (1000 mg/L). In contrast, ZnO, Mn_2O_3, and Ag^0 nanoparticles caused a pronounced decrease in the CI at very low concentrations. Figure 1 shows the response of 16HBE14o- cells to different nanomaterials (CeO_2, Al_2O_3, SiO_2, and Mn_2O_3) as a function of time as determined in the RTCA assay. RTCA traces obtained for other nanomaterials found to elicit dose–response effects are provided in the Supporting Information (SI) section. Figure 1A illustrates the response of RTCA to a nontoxic NP, such as CeO_2 with no adverse effect at concentrations up to 1000 mg/L. On the other hand, Al_2O_3, SiO_2, and Mn_2O_3 NPs caused toxicity to the cells, as indicated by a considerable decrease in the CI with increasing NP concentration (Figure 1B, 1C, and 1D, respectively). Mn_2O_3 NPs displayed the highest toxicity among the NPs illustrated in Figure 1, showing inhibitory effects at concentrations as low as 20 mg/L. SiO_2 and Al_2O_3 were moderately toxic with substantial decreases in the CI being observable at concentrations exceeding 200 and 250 mg/L, respectively. Cell-free controls confirmed that none of the NPs interfered with the impedance measurements even at the highest concentrations used.

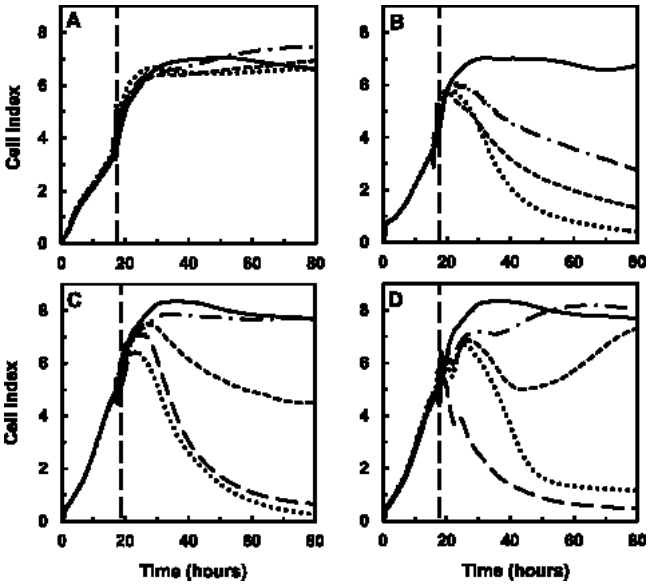

Figure 1. Dynamic monitoring of the cytotoxic response of human bronchia epithelial cells (16HBE14o-) exposed to different concentrations of inorganic NPs using the RTCA system. Panel A: Nano-CeO_2 concentrations (mg/L): 0 (—), 250 (— • —), 500 (- - -), and 1000 (•••••••). Panel B: Nano-Al_2O_3 (mg/L): 0 (—), 250 (— • —), 500 (- - -), and 1000 (•••••••). Panel C: Nano-SiO_2 (mg/L): 0 (—), 100 (— • —), 200 (- - -), 300 (•••••••), and 600 (— —). Panel D: Nano-Mn_2O_3 (mg/L): 0 (—), 10 (— • —), 20 (- - -), 50 (•••••••), and 100 (— —).

The RTCA output is dynamic, enabling measurement of cytotoxicity that may significantly change over time as exemplified in the case of Mn_2O_3 NPs (Figure 1D). Therefore, to facilitate treatment comparisons, a normalized response was calculated at 48 h of exposure to the NPs. Figure 2 summarizes

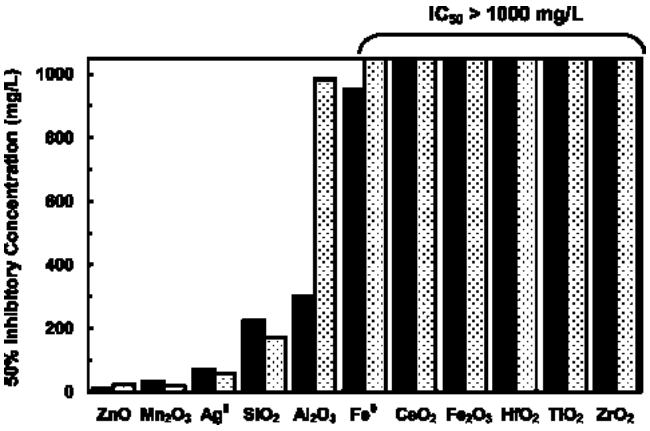

Figure 2. Concentration of the inorganic NPs investigated causing 50% inhibition toward human bronchial epithelial cells (16HBE14o-) after 48 h of exposure in the RTCA assay (solid bar) and MTT assay (dotted bar).

the 50% inhibitory concentration (IC_{50}) values obtained with 48 h normalized cell toxicity data. ZnO, Mn_2O_3, and Ag^0 NPs were the most highly toxic with IC_{50} values as low as 13, 33, and 72 mg/L, respectively. SiO_2 and Al_2O_3 NPs were moderately toxic with IC_{50} values of several hundred mg/L. Finally, the remaining NPs tested displayed no toxicity within

the dose range tested (CeO_2, TiO_2, HfO_2, ZrO_2, and Fe_2O_3), or very low toxicity (Fe^0).

The impedance-based RTCA system has a demonstrated applicability to evaluate the cytotoxicity of a variety of dissolved chemicals.[10,19,20] However, information on the suitability of this novel technique for nanotoxicity assessment is very limited. To our knowledge, this is the first time that the RTCA system has been applied to evaluate the cytotoxicity of a suite of inorganic NPs. The results obtained show that the RTCA can successfully be applied to test different inorganic NPs for potential cytotoxicity to human bronchial epithelial 16HBE14o- cells. For example, when the cytotoxicity of micro- and nano-SiO_2 to mouse macrophages (RAW264.7) was evaluated with RTCA, SiO_2 NPs were shown to be cytotoxic at concentrations around 300 mg/L.[15] Additionally, evaluation of NP cytotoxicity on A549 cells (a human lung epithelial cell line generated from the alveolus) showed distinct cytotoxicity for ZnO and negligible effects for TiO_2 NPs,[21] which is consistent with our results.

In addition to being a high throughput method, RTCA is information rich, providing insight on how cells are responding over time. The capture of dynamic behavior can be viewed as a real advantage over conventional cytotoxicity assays that tend to rely on a single end-point. The RTCA analyzer detects cellular changes that may affect to their adhesion to the E-plate, such as cell number, viability, and morphological modifications. The impedance measurements provide information on the overall status of the cells when exposed to the NPs and allow the detection of cellular signaling and intermediate cytotoxic responses that are largely missed in end-point analyses. However, because the RTCA analysis reports a physiological interaction, that is, interaction of the cell with the plate electrode, specific mechanisms of toxicity are not immediately evident from high throughput experiments. To validate that the CI responses determined here using the RTCA system were truly due to cytotoxicity, the conventional MTT assay was used with the same suite of NPs.

Cytotoxicity Assessment Using the MTT Assay. The NPs utilized in this study were tested for toxicity toward 16HBE14o- cells using the MTT assay. Unlike the RTCA data shown above, the MTT has a known biochemical mechanism based on the activity of mitochondrial reductases.[22] Comparable to the behavior detected using the RTCA system, the most toxic NPs were ZnO, Mn_2O_3, and Ag^0; whereas, CeO_2, TiO_2, HfO_2, ZrO_2, and Fe_2O_3 caused little inhibition at the maximum concentration tested (1000 mg/L). Figure 3 shows typical absorbance readings obtained in the MTT analysis with nanosized Al_2O_3, SiO_2, and Mn_2O_3. In all cases, a significant decrease in the absorbance values was observed after the cells were exposed to NPs, which indicates a decrease in the mitochondrial activity of the cells. The mitochondrial activity of 16HBE14o- cells exposed to 1000 mg/L of Al_2O_3 was 49% of the maximum activity detected for the NP-free control (Figure 3A). This decline was sharper when the cells were exposed to SiO_2 and Mn_2O_3 NPs (Figures 3B and 3C, respectively). SiO_2 at 1,000 mg/L reduced the activity by 79%. Mn_2O_3 caused almost complete inhibition at lower concentrations (88% reduction at 500 mg/L).

Several studies have reported that NPs can cause interference in the MTT assay.[7,23] As an example, ZnO NPs interfered with MTT readings. However, the interference was reduced when the cells were washed twice with PBS prior to the addition of the MTT-medium solution or when an alternative solvent was used.[23] In this study, cells were washed twice with PBS before the addition of the MTT-medium solution to enhance NP removal. In addition, cell-free controls supplied with the highest concentration of NPs tested were run in parallel to all the assays to check for interference of the NPs with the absorbance readings. Comparison of the cell-free controls with and without NPs (treatments C1 and C2 in Figure 3) revealed that there was minor (negligible) interference of the NPs with the absorbance readings.

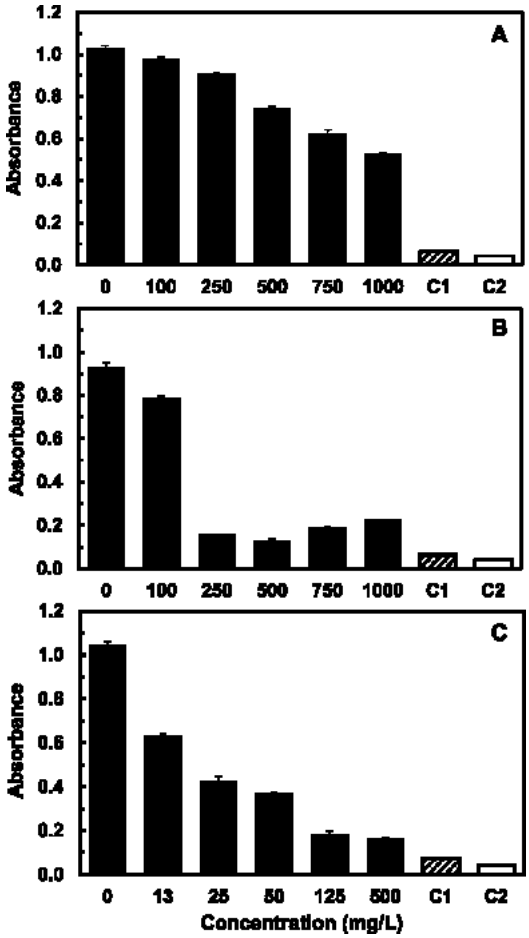

Figure 3. Absorbance readings obtained with the MTT assay using human bronchial epithelial cells (16HBE14o-) exposed for 48 h to different concentrations of nano-Al_2O_3 (Panel A), nano-SiO_2 (Panel B), and nano-Mn_2O_3 (Panel C). Legends: Cells exposed to NPs (solid bar); Cell-free controls with maximum concentration of NPs (1,000 mg Al_2O_3/L, 1,000 mg SiO_2/L, and 500 mg Mn_2O_3/L, respectively) (C1, slashed bar); NP- and cell-free control with DMSO (C2, open bar).

In contrast with the limited information on the applicability of the RTCA system to evaluate nanotoxicity, the MTT assay is frequently used to assess the cytotoxicity of NPs toward different mammalian cells. Different MTT studies have consistently reported moderate toxicity for SiO_2,[15,24] and high toxicity for ZnO NPs[25,26] as well as Ag^0 NPs[27,28] to human or mouse pulmonary cell lines. SiO_2 has been reported to cause lipid peroxidation and membrane damage to A549 cells produced by oxidative stress.[24] Both, ZnO and Ag^0 were identified to cause reactive oxygen species (ROS) formation and cell death.[26,28] Moreover, the release of toxic ions by ZnO NPs is usually related to its cytotoxic effects.[29] However, that is not the case in the present study, in which the concentrations of soluble Zn^{2+} detected were negligible in the medium utilized.

On the other hand, HfO_2 NPs at concentrations as high as 2000 mg/L caused only minor inhibition to human urothelial cells (UROtsa) assessed by the MTT,[30] which agrees with the lack of cytotoxicity observed in the present study.

Literature results for the other NPs tested in this study are conflicting. Most MTT studies agree that nano-Al_2O_3 has inhibitory impacts to cells. However, the extent of the adverse effects varies depending on the study. Elevated cytotoxicity of nano-Al_2O_3 ($IC_{50} \approx 5$ mg/L) was observed with human alveolar macrophage cells THB-1 exposed for 48 h.[31] In contrast, another MTT study conducted with cells exposed for 24 h to nano-Al_2O_3 provided disparate values (IC_{50} values of 82 and 866 mg/L) from two different laboratories.[25] Finally, CeO_2, TiO_2, Fe_2O_3, and ZrO_2 NPs, which displayed low- or no toxicity in the present study, have been found in some cases to cause moderate toxicity to different mammalian cell lines.[25,26,31,32]

Previous studies have not evaluated the inhibition caused by Mn_2O_3 and Fe^0 NPs with the MTT test. Likewise, not much is known regarding the toxicity of nano-Mn_2O_3 to human cells using other assays. The high cytotoxicity caused by Mn_2O_3 in the present study could be due to ROS. Mn oxides appear to promote chemical and biological ROS generation. Different Mn oxide NPs have been identified as ROS inducers in lung cells as well as in neuronal cells at relatively low concentrations.[33−35] In a recent study, nano-Mn_2O_3 was also shown to have a high oxidant capability as demonstrated by its ability to directly oxidize a ROS-indicator dye.[36] ROS generation could also account for the moderate cytotoxicity observed with Fe^0 in the present study. ROS production by 16HBE14o- cells exposed to Fe^0 NPs has been detected.[37] In this respect, it is interesting to note that fresh Fe^0 NPs was recently shown to cause oxidative stress and other cytotoxic effects on mammalian cells (rodent microglia (BV2) and neuron cells (N27)).[38] The authors reported a sharp decrease in the cytotoxicity of nano-Fe with material aging.

Correlation between RTCA and MTT Results. Figure 4 shows the dose−response curves determined for 16HBE14o- cells after 48-h exposure to different concentrations of nanosized Al_2O_3, SiO_2, and Mn_2O_3 using the RTCA and MTT assays. To compare the results obtained with both assays, the normalized response from RTCA relative to that of the NP-free control was calculated after 48 h of exposure to NPs (eq 3). An excellent correlation was observed between the results obtained for SiO_2 and Mn_2O_3 NPs by both bioassays. As an example, the 50% ICs determined by the RTCA and MTT method were very close, 33 and 18 mg/L for Mn_2O_3, and 225 and 172 mg/L for SiO_2, respectively (Figure 2). In the case of Al_2O_3, the inhibitory values determined differed significantly (Figure 4A); although, both assays indicated that this NP was only moderately toxic. For instance, the IC_{50} determined for Al_2O_3 using the RTCA and MTT assays were 301 and 984 mg/L, respectively. The cytotoxicity results determined for the other inorganic NPs using the RTCA and the MTT were highly correlated, as shown in Figure 2. ZnO and Ag^0 displayed high toxicity at low concentrations, causing 50% inhibition at 13 and 22 mg/L (ZnO), and 72 and 59 mg/L (Ag^0), using the RTCA and MTT method, respectively (Figure 2). Other NPs, such as Fe^0, Fe_2O_3, HfO_2, TiO_2, and ZrO_2, presented similar tendencies causing very low inhibition (Fe^0) or no inhibition (CeO_2, Fe_2O_3, HfO_2, TiO_2, and ZrO_2) at concentrations of up to 1000 mg/L (Figure 2).

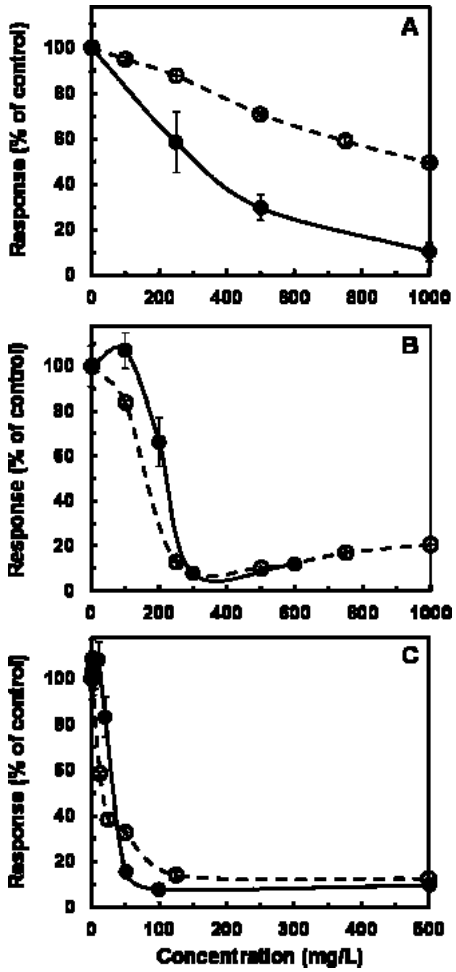

Figure 4. Percent of response measured by RTCA assay (●) or MTT assay (○) on human bronchial epithelial cells (16HBE14o-) exposed for 48 h to nano-Al_2O_3 (Panel A), nano-SiO_2 (Panel B), and nano-Mn_2O_3 (Panel C). Response data are expressed as percentage of the response obtained in the respective NPs-free controls.

This is the first study evaluating and demonstrating an excellent correlation between RTCA and a physiological based toxicity assay (MTT) for inorganic NPs. A good correspondence between the two bioassays has been reported in previous studies for different dissolved organic and inorganic compounds. An excellent correlation between RTCA and MTT cytotoxicity data was found for soluble inorganic compounds like arsenic, mercury, and sodium dichromate toward different cell lines.[10] Other studies using organic compounds like quercetin or carbon nanotubes (CNT) found similar correlation between RTCA and MTT results.[19,20] However, in a cell proliferation study in which the authors evaluated the correspondence between CI and cell number, the correlation between RTCA and MTT was shown to be cell dependent, since the results only corresponded well for three of the four cell lines tested.[39] The disparity in the severity of the Al_2O_3 NPs responses observed in this study might be due to complex biological changes detected by the RTCA system. The impedance-based system detects combinatory physiological changes between adherent cells and the electrodes that line their substrate while the MTT test specifically detects the respiratory activity of the mitochondria. Subtle membrane altering effects, such as cell spreading, reduced adherence at cell/substrate contacts, or membrane depolarization induced by

Table 1. Average Particle Size and ζ-Potential of the Nanomaterials Investigated Following Dilution of the Various Stock Dispersions (2000 mg NP/L) in Culture Medium Containing MEM with 5% FBS (Final Dilution = 1:3, v/v) and Static Incubation for 24 h at 37°C[a]

		average hydrodynamic size (nm)		average zeta potential (mV)	
NP	manufacturer reported particle size (nm)	total[b]	supernatant	total	supernatant
Ag^{0c}	<100	171 ± 2	133 ± 4	−12.1 ± 1.0	−11.6 ± 0.6
Al_2O_3	<50	164 ± 28	90 ± 1	−14.7 ± 0.8	−14.2 ± 0.6
CeO_2	<50	189 ± 7	193 ± 13	−13.9 ± 0.5	−12.5 ± 0.5
SiO_2	10−20	1,142 ± 88	549 ± 61	−12.8 ± 0.8	−11.7 ± 1.3
HfO_2	100	212 ± 4	190 ± 13	−13.6 ± 0.6	−13.0 ± 1.2
ZrO_2	20−30	585 ± 9	278 ± 13	−12.8 ± 1.1	−11.4 ± 0.2
TiO_2	25	634 ± 17	293 ± 85	−12.9 ± 1.0	−13.3 ± 0.6
ZnO	10−30	2,776 ± 307	262 ± 46	−11.0 ± 0.6	−10.5 ± 1.0
Fe^0	40−60	2,917 ± 328	21 ± 5	−12.5 ± 0.5	−9.0 ± 1.9
Fe_2O_3	40−60	201 ± 6	182 ± 5	−13.0 ± 0.3	−13.4 ± 1.2
Mn_2O_3	40−60	1,172 ± 59	588 ± 17	−14.4 ± 0.8	−15.4 ± 0.5

[a]The particle size reported by the NP supplier is compared with the average hydrodynamic diameter determined in samples of the corresponding supernatant and mixed whole sample. [b]Whole mixed dispersion. [c]0.2% polyvinylpyrrolidone (PVP) coated.

short-term exposure to Al_2O_3 NPs as reported in the A549 human lung derived cell line,[40] are specific examples of processes that might contribute to RTCA results but not MTT.

In conclusion, this study demonstrated an excellent correlation between RTCA and a physiological based toxicity assay (MTT) for inorganic NPs. A distinct advantage of RTCA is its capability to continuously monitor the response of live cells to NP exposure over time. This allows for the detection of dynamic toxic effects that may be overlooked in common end-point analyses.[10]

Aggregation of Nanoparticles in Biological Medium. The stability of the different NPs in the bioassay medium used in this study was evaluated by determining the particle size distribution (PSD), ζ-potential, and the concentration of NPs remaining in suspension after 24 h of incubation (37 °C, 5% CO_2). All NPs, with the exception of CeO_2, Al_2O_3, and SiO_2 showed a high tendency to aggregate in the growth medium. Nanosized ZnO agglomerated the most, as indicated by the high average aggregate particle size determined, 2,776 nm (Table 1), which corresponds to an increase of 90- to 275-fold over the primary particle size (10−30 nm). The high average agglomerate diameters determined for Fe^0 and Mn_2O_3, 2,917 and 1,172 nm, respectively, also indicate significant aggregation of these two nanomaterials in the bioassay medium. Other compounds (TiO_2, Fe_2O_3, HfO_2, and ZrO_2) agglomerated to a lower extent, resulting in average aggregate diameters ranging from 200 to 600 nm. The ζ-potential measurements (Table 1) indicating low surface charge also support the tendency for aggregation of these nanomaterials in the medium. The agglomeration of NPs led to a decrease in the concentration effectively dispersed, as confirmed by the measurement of the concentration of NPs remaining in suspension after 24 h of incubation. As much as 90−100% of the initial amount of ZnO, Fe^0, Mn_2O_3, TiO_2, Fe_2O_3, HfO_2, and ZrO_2 NPs settled after 24 h (Figure 5).

In contrast, CeO_2, Al_2O_3, and SiO_2 NPs displayed high stability in the medium. Although the increase in average particle size is significant compared to the diameters reported by the supplier (about 3−4 times), the average CeO_2 aggregate size determined in both the supernatant and in the whole mixed suspension (~190 nm) were very similar. The extraordinary stability of nano-CeO_2 in the bioassay medium was confirmed by the high levels of the nanomaterial remaining (~90%) in suspension after 24 h of incubation in MEM containing 5% of FBS (Figure 5). Nano-Al_2O_3 dispersions were also quite stable; even though the aggregate size determined in the mixed dispersion (164 nm) was 2-fold higher than that in the supernatant (90 nm), 63% of the initially added nanomaterial remained in suspension after 24 h of incubation in the medium. Finally, nano-SiO_2 formed quite large aggregates (549 nm average size in the supernatant) which, however, showed high stability in the medium (69% remaining after 24 h).

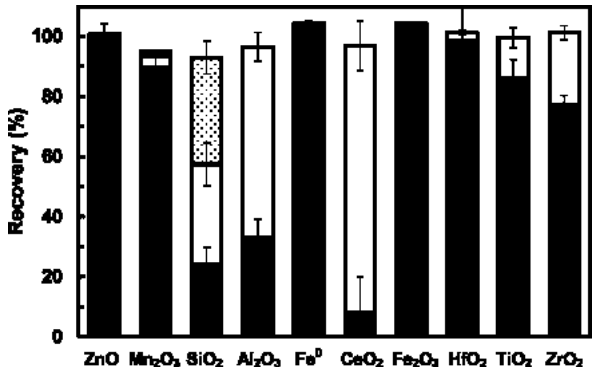

Figure 5. Distribution of inorganic nanomaterials in different fractions: settled (solid bar), suspended (open bar), and soluble (dotted bar), as percentage of the initial concentration added, following dilution of the NP stocks (2,000 mg/L) in culture medium containing MEM with 5% FBS (final dilution = 1:3, v/v) and subsequent static incubation (37 °C, 5% CO_2) for 24 h.

The high tendency of most NPs tested to aggregate and settle out of the bioassay medium is in agreement with several studies showing destabilization of NP dispersions in the media used in various toxicity tests.[41,42] The extent of aggregation is not only dependent on the properties of the particle (shape, size, surface area, etc.) but it is also strongly dependent on the presence of other dissolved compounds like salts or organics in the medium.[43] The medium used in the cytotoxicity assays (MEM containing 5% of FBS) includes different salts that can play a destabilizing role by increasing the ionic strength of the mixture, as has been demonstrated for several inorganic NPs.[44,45] On the other hand, the medium also contains proteins (e.g., FBS) that may selectively enhance the dispersion of some nanomaterials, such as CeO_2 and Al_2O_3.

Aggregation and settling of NPs during in vitro cytotoxicity testing is a concern because of the possibility of increasing the local concentration of NPs, potentially causing misleading results.[46] Formation of large aggregates exceeding the typical dimensions of NPs (1−100 nm) also may preclude the evaluation of nanotoxicity. However, the extent to which primary particles may again disperse once they contact or are taken up by cells is not well-known. Different methods have been used to improve the dispersion of NPs including the use of ultrasound energy, as in the present work, and with the use of chemical or biological dispersants.[47] Dispersants have the advantage of being very effective even in the long term. However it is difficult, if not impossible, to find a biocompatible and universal dispersant that is effective for all types of NPs.

■ ASSOCIATED CONTENT

Supporting Information

List of the main chemicals used, acid digestion mixtures and conditions, wavelengths used and detection limits in the ICP-OES analyses, TEM images of the nanomaterials investigated, and additional figures obtained with the RTCA for Ag^0 and ZnO NPs. This material is available free of charge via the Internet at http://pubs.acs.org.

■ AUTHOR INFORMATION

Corresponding Author

*Phone: +1-520-626-2829. Fax: +1-520-621-6048. E-mail: rsierra@email.arizona.edu.

Notes

The authors declare no competing financial interest.

■ ACKNOWLEDGMENTS

This work was supported by a grant from the SRC/Sematech Engineering Research Center for Environmentally Benign Semiconductor Manufacturing.

■ REFERENCES

(1) Savolainen, K.; Pylkkanen, L.; Norppa, H.; Falck, G.; Lindberg, H.; Tuomi, T.; Vippola, M.; Alenius, H.; Hameri, K.; Koivisto, J.; Brouwer, D.; Mark, D.; Bard, D.; Berges, M.; Jankowska, E.; Posniak, M.; Farmer, P.; Singh, R.; Krombach, F.; Bihari, P.; Kasper, G.; Seipenbusch, M. Nanotechnologies, engineered nanomaterials and occupational health and safety—A review. *Saf. Sci.* **2010**, *48* (8), 957−963.

(2) Ju-Nam, Y.; Lead, J. R. Manufactured nanoparticles: An overview of their chemistry, interactions and potential environmental implications. *Sci. Total Environ.* **2008**, *400* (1−3), 396−414.

(3) Yang, Z. H.; Zhang, Y. C.; Zhang, W. X.; Wang, X.; Qian, Y. T.; Wen, X. G.; Yang, S. H. Nanorods of manganese oxides: Synthesis, characterization and catalytic application. *J. Solid State Chem.* **2006**, *179* (3), 679−684.

(4) Golden, J. H.; Small, R.; Pagan, L.; Shang, C.; Raghavan, S. Evaluating and treating CMP wastewater. *Semicond. Int.* **2000**, *23* (12), 85−98.

(5) Gottschalk, F.; Nowack, B. The release of engineered nanomaterials to the environment. *J. Environ. Monit.* **2011**, *13* (5), 1145−1155.

(6) Worle-Knirsch, J. M.; Pulskamp, K.; Krug, H. F. Oops they did it again! Carbon nanotubes hoax scientists in viability assays. *Nano Lett.* **2006**, *6* (6), 1261−1268.

(7) Fisichella, M.; Dabboue, H.; Bhattacharyya, S.; Saboungi, M. L.; Salvetat, J. P.; Hevor, T.; Guerin, M. Mesoporous silica nanoparticles enhance MTT formazan exocytosis in HeLa cells and astrocytes. *Toxicol. In Vitro* **2009**, *23* (4), 697−703.

(8) Aam, B. B.; Fonnum, F. Carbon black particles increase reactive oxygen species formation in rat alveolar macrophages in vitro. *Arch. Toxicol.* **2007**, *81* (6), 441−446.

(9) Atienza, J. M.; Yu, N. C.; Kirstein, S. L.; Xi, B.; Wang, X. B.; Xu, X.; Abassi, Y. A. Dynamic and label-free cell-based assays using the real-time cell electronic sensing system. *Assay Drug Dev. Technol.* **2006**, *4* (5), 597−607.

(10) Xing, J. Z.; Zhu, L.; Jackson, J. A.; Gabos, S.; Sun, X.-J.; Wang, X.-b.; Xu, X. Dynamic monitoring of cytotoxicity on microelectronic sensors. *Chem. Res. Toxicol.* **2005**, *18* (2), 154−161.

(11) Damoiseaux, R.; George, S.; Li, M.; Pokhrel, S.; Ji, Z.; France, B.; Xia, T.; Suarez, E.; Rallo, R.; Madler, L.; Cohen, Y.; Hoek, E. M. V.; Nel, A. No time to lose-high throughput screening to assess nanomaterial safety. *Nanoscale* **2011**, *3* (4), 1345−1360.

(12) Huang, L.; Xie, L.; Boyd, J. M.; Li, X.-F. Cell-electronic sensing of particle-induced cellular responses. *Analyst* **2008**, *133* (5), 643−648.

(13) Wu, C. H.; Shi, L. X.; Li, Q. N.; Jiang, H.; Selke, M.; Ba, L.; Wang, X. M. Probing the dynamic effect of cys-CdTe quantum dots toward cancer cells in vitro. *Chem. Res. Toxicol.* **2010**, *23* (1), 82−88.

(14) Mu, Q. X.; Yang, L.; Davis, J. C.; Vankayala, R.; Hwang, K. C.; Zhao, J. C.; Yan, B. Biocompatibility of polymer grafted core/shell iron/carbon nanoparticles. *Biomaterials* **2010**, *31* (19), 5083−5090.

(15) Yang, H.; Wu, Q. Y.; Tang, M.; Liu, X.; Deng, H. H.; Kong, L.; Lu, Z. H. In vitro study of silica nanoparticle-induced cytotoxicity based on real-time cell electronic sensing system. *J. Nanosci. Nanotechnol.* **2010**, *10* (1), 561−568.

(16) Cozens, A. L.; Yezzi, M. J.; Kunzelmann, K.; Ohrui, T.; Chin, L.; Eng, K.; Finkbeiner, W. E.; Widdicombe, J. H.; Gruenert, D. C. CFTR expression and chloride secretion in polarized immortal human bronchial epithelial-cells. *Am. J. Respir. Cell Mol. Biol.* **1994**, *10* (1), 38−47.

(17) Flynn, A. N.; Tillu, D. V.; Asiedu, M. N.; Hoffman, J.; Vagner, J.; Price, T. J.; Boitano, S. The protease-activated receptor-2-specific agonists 2-aminothiazol-4-yl-LIGRL-NH2 and 6-aminonicotinyl-LIGRL-NH2 stimulate multiple signaling pathways to induce physiological responses in vitro and in vivo. *J. Biol. Chem.* **2011**, *286* (21), 19076−19088.

(18) Eaton, A. D.; Franson, M. A. H. *Standard Methods for the Examination of Water & Wastewater*; American Public Health Association: Washington, DC, 2005.

(19) Guo, D. D.; Wu, C. H.; Li, J. Y.; Guo, A. R.; Li, Q. N.; Jiang, H.; Chen, B. A.; Wang, X. M. Synergistic effect of functionalized nickel nanoparticles and quercetin on inhibition of the SMMC-7721 cells proliferation. *Nanoscale Res. Lett.* **2009**, *4* (12), 1395−1402.

(20) Ren, D.-M.; Li, M.; Dong, Y.-Y.; Cheng, Y.; Yang, X.-R.; Zou, Y.-D.; Zheng, H.-Y.; Bai, H.; Chu, X.-G.; Wang, J.-B. Realtime cytotoxicity characterization with cell-microelectronic sensing of water soluble carbon nanotubes. *Synth. React. Inorg., Met.−Org., Nano−Met. Chem.* **2009**, *39* (9), 600−604.

(21) Seiffert, J. M.; Baradez, M. O.; Nischwitz, V.; Lekishvili, T.; Goenaga-Infante, H.; Marshall, D. Dynamic monitoring of metal oxide nanoparticle toxicity by label free impedance sensing. *Chem. Res. Toxicol.* **2012**, *25* (1), 140−152.

(22) Mosmann, T. Rapid colorimetric assay for cellular growth and survival - Application to proliferation and cyto-toxicity assays. *J, Immunol. Methods* **1983**, *65* (1−2), 55−63.

(23) Hsiao, I. L.; Huang, Y. J. Improving the interferences of methyl thiazolyl tetrazolium and IL-8 assays in assessing the cytotoxicity of nanoparticles. *J. Nanosci. Nanotechnol.* **2011**, *11* (6), 5228−5233.

(24) Akhtar, M. J.; Ahamed, M.; Kumar, S.; Siddiqui, H.; Patil, G.; Ashquin, M.; Ahmad, I. Nanotoxicity of pure silica mediated through oxidant generation rather than glutathione depletion in human lung epithelial cells. *Toxicology* **2010**, *276* (2), 95−102.

(25) Lanone, S.; Rogerieux, F.; Geys, J.; Dupont, A.; Maillot-Marechal, E.; Boczkowski, J.; Lacroix, G.; Hoet, P. Comparative toxicity of 24 manufactured nanoparticles in human alveolar epithelial and macrophage cell lines. *Part. Fibre Toxicol.* **2009**, *6* (1), 14.

(26) Hsiao, I. L.; Huang, Y. J. Effects of various physicochemical characteristics on the toxicities of ZnO and TiO(2) nanoparticles

toward human lung epithelial cells. *Sci. Total Environ.* **2011**, *409* (7), 1219−1228.
(27) Foldbjerg, R.; Dang, D.; Autrup, H. Cytotoxicity and genotoxicity of silver nanoparticles in the human lung cancer cell line, A549. *Arch. Toxicol.* **2010**, *85* (7), 743−750.
(28) Liu, W.; Wu, Y.; Wang, C.; Li, H. C.; Wang, T.; Liao, C. Y.; Cui, L.; Zhou, Q. F.; Yan, B.; Jiang, G. B. Impact of silver nanoparticles on human cells: Effect of particle size. *Nanotoxicology* **2010**, *4* (3), 319−330.
(29) Xia, T.; Kovochich, M.; Liong, M.; Madler, L.; Gilbert, B.; Shi, H. B.; Yeh, J. I.; Zink, J. I.; Nel, A. E. Comparison of the mechanism of toxicity of zinc oxide and cerium oxide nanoparticles based on dissolution and oxidative stress properties. *ACS Nano* **2008**, *2* (10), 2121−2134.
(30) Field, J. A.; Luna-Velasco, A.; Boitano, S. A.; Shadman, F.; Ratner, B. D.; Barnes, C.; Sierra-Alvarez, R. Cytotoxicity and physicochemical properties of hafnium oxide nanoparticles. *Chemosphere* **2011**, *84* (10), 1401−1407.
(31) Soto, K.; Garza, K. M.; Murr, L. E. Cytotoxic effects of aggregated nanomaterials. *Acta Biomater.* **2007**, *3* (3), 351−358.
(32) Park, E.-J.; Choi, J.; Park, Y.-K.; Park, K. Oxidative stress induced by cerium oxide nanoparticles in cultured BEAS-2B cells. *Toxicology* **2008**, *245* (1−2), 90−100.
(33) Choi, J.; Lee, S.; Na, H.; An, K.; Hyeon, T.; Seo, T. In vitro cytotoxicity screening of water-dispersible metal oxide nanoparticles in human cell lines. *Bioprocess Biosyst. Eng.* **2009**, *33* (1), 21−30.
(34) Hussain, S. M.; Javorina, A. K.; Schrand, A. M.; Duhart, H. M.; Ali, S. F.; Schlager, J. J. The interaction of manganese nanoparticles with PC-12 cells induces dopamine depletion. *Toxicol. Sci.* **2006**, *92* (2), 456−463.
(35) Stefanescu, D.; Khoshnan, A.; Patterson, P.; Hering, J. Neurotoxicity of manganese oxide nanomaterials. *J. Nanopart. Res.* **2009**, *11* (8), 1957−1969.
(36) Luna-Velasco, A.; Field, J. A.; Cobo-Curiel, A.; Sierra-Alvarez, R. Inorganic nanoparticles enhance the production of reactive oxygen species (ROS) during the autoxidation of L-3,4-dihydroxyphenylalanine (L-dopa). *Chemosphere* **2011**, *85* (1), 19−25.
(37) Keenan, C. R.; Goth-Goldstein, R.; Lucas, D.; Sedlak, D. L. Oxidative stress induced by zero-valent iron nanoparticles and Fe(II) in human bronchial epithelial cells. *Environ. Sci. Technol.* **2009**, *43* (12), 4555−4560.
(38) Phenrat, T.; Long, T. C.; Lowry, G. V.; Veronesi, B. Partial oxidation ("aging") and surface modification decrease the toxicity of nanosized zerovalent iron. *Environ. Sci. Technol.* **2009**, *43* (1), 195−200.
(39) Vistejnova, L.; Dvorakova, J.; Hasova, M.; Muthny, T.; Velebny, V.; Soucek, K.; Kubala, L. The comparison of impedance-based method of cell proliferation monitoring with commonly used metabolic-based techniques. *Neuroendocrinol. Lett.* **2009**, *30*, 121−127.
(40) Lin, W.; Stayton, I.; Huang, Y.-w.; Zhou, X.-D.; Ma, Y. Cytotoxicity and cell membrane depolarization induced by aluminum oxide nanoparticles in human lung epithelial cells A549. *Toxicol. Environ. Chem.* **2008**, *90* (5), 983−996.
(41) Murdock, R. C.; Braydich-Stolle, L.; Schrand, A. M.; Schlager, J. J.; Hussain, S. M. Characterization of nanomaterial dispersion in solution prior to In vitro exposure using dynamic light scattering technique. *Toxicol. Sci.* **2008**, *101* (2), 239−253.
(42) Allouni, Z. E.; Cimpan, M. R.; Hol, P. J.; Skodvin, T.; Gjerdet, N. R. Agglomeration and sedimentation of TiO(2) nanoparticles in cell culture medium. *Colloids Surf., B* **2009**, *68* (1), 83−87.
(43) Handy, R.; Owen, R.; Valsami-Jones, E. The ecotoxicology of nanoparticles and nanomaterials: current status, knowledge gaps, challenges, and future needs. *Ecotoxicology* **2008**, *17* (5), 315−325.
(44) French, R. A.; Jacobson, A. R.; Kim, B.; Isley, S. L.; Penn, R. L.; Baveye, P. C. Influence of ionic strength, pH, and cation valence on aggregation kinetics of titanium dioxide nanoparticles. *Environ. Sci. Technol.* **2009**, *43* (5), 1354−1359.
(45) El Badawy, A. M.; Luxton, T. P.; Silva, R. G.; Scheckel, K. G.; Suidan, M. T.; Tolaymat, T. M. Impact of environmental conditions (pH, ionic strength, and electrolyte type) on the surface charge and aggregation of silver nanoparticles suspensions. *Environ. Sci. Technol.* **2010**, *44* (4), 1260−1266.
(46) Cho, E. C.; Zhang, Q.; Xia, Y. N. The effect of sedimentation and diffusion on cellular uptake of gold nanoparticles. *Nat. Nanotechnol.* **2011**, *6* (6), 385−391.
(47) Bihari, P.; Vippola, M.; Schultes, S.; Praetner, M.; Khandoga, A. G.; Reichel, C. A.; Coester, C.; Tuomi, T.; Rehberg, M.; Krombach, F. Optimized dispersion of nanoparticles for biological in vitro and in vivo studies. *Part. Fibre Toxicol.* **2008**, *5*, 14.